ELSEVIER

Catalysis Today 65 (2001) 201–208

CATALYSIS TODAY

www.elsevier.com/locate/cattod

Characterisation of bimetallic platinum systems: application to the reduction of aromatics in presence of sulfur

E. Guillon*, J. Lynch, D. Uzio, B. Didillon

Institut Français du Pétrole, 1 and 4 Av de Bois Préau, 92852 Rueil-Malmaison, France

Abstract

Hydrogenation activity in presence of sulfur has been studied for bimetallic Pt–Ge/Al_2O_3 and Pt–Pd/Al_2O_3 systems. It has been shown that addition of germanium to platinum decreases the rate of aromatic hydrogenation whereas the palladium–platinum system exhibits higher activity. On the basis of a precise description of physico-chemical properties of bimetallic particles (characterisation by TEM, EXAFS, LEIS, TPR), a concept of sulfur resistant catalyst is discussed taking into account each actor in the catalytic process and their role in the modification of the active site properties.

Keywords: Sulfur resistance; Platinum; Aromatics reduction; Bimetallic

1. Introduction

Supported platinum clusters are well known for their high activity in the reduction of aromatic carbons. For industrial applications, the main drawback of such catalytic systems is their high sensitivity to sulfur remaining in the fuels. Recently, many studies have been dedicated to this problem and improvements of the sulfur resistance have been observed by varying the acidity of the support or by adding a second metal [1–4]. Nevertheless, the real parameter governing the sulfur resistance is still unclear [5], even if electro-deficiency of metal atoms is often proposed to have the effect of weakening the metal–sulfur bond [6–9]. Some contradictions in the literature exist about the sulfur resistance of metallic catalysts. This present work is an attempt to elucidate the effect and the role of the second metal in alumina supported platinum–germanium and platinum–palladium catalysts.

2. Experimental

2.1. Preparation of catalysts

The support used was a γ-alumina with a specific surface area of 200 m^2/g and a pore volume of 0.6 g/cm^3. The monometallic catalysts Pt_1 and Pd_1 were obtained by incipient wetness impregnation of alumina with platinum bis-acetylacetonate $Pt(Acac)_2$ or palladium bis-acetylacetonate $Pd(Acac)_2$ in toluene according to the procedure described by Merlen et al. [10]. Pt–Ge/Al_2O_3 catalysts were prepared by incipient wetness impregnation by mixing the monometallic parent catalyst Pt_1 (1.02 wt.% Pt) with appropriate amounts of tetra-*n*-butyl germane $Ge(C_4H_9)_4$ dissolved in *n*-heptane. After drying 12 h at 120°C, the catalyst was reduced 2 h at 450°C under hydrogen flow. Bimetallic catalysts are referred to Pt_xGe_y in

* Corresponding author.
E-mail address: emmannell.GUILLON@ifp.fr (E. Guillon).

0920-5861/01/$ – see front matter
PII: S0920-5861(00)00565-4

this work. Pt–Pd/Al_2O_3 catalysts were prepared by coimpregnation of $Pt(Acac)_2$ and $Pd(Acac)_2$. The two complexes were dissolved in toluene. The mixture was put in contact with alumina during 72 h at room temperature and activated under air flow at 350°C during 2 h and then reduced 2 h at 450°C under hydrogen flow. The catalysts prepared by this method are called Pt_xPd_yco.

2.2. Catalytic tests

Orthoxylene hydrogenation reaction was chosen as test reaction and performed with and without addition of sulfur compound in the feed.

Without sulfur addition. The test was performed in a continuous fixed-bed reactor under atmospheric pressure. Operating conditions were as follows: catalyst (2 g), $T = 100$°C, 120 ml h^{-1} of feed (10 wt.% of orthoxylene in *n*-heptane), 6 l h^{-1} of H_2.

With addition of sulfur compounds. The test was performed in a continuous fixed-bed reactor under a total pressure of 40 bar. Feed was composed of orthoxylene (10 wt.%) in *n*-heptane. Sulfur (100 ppm) was added as dimethyl disulphide (DMDS). Operating conditions were as follows: during 10 h at 20 l h^{-1} of H_2, $T = 100$°C, LHSV = 7 h^{-1} then during 20 h at $T = 100$°C and LHSV = 1 h^{-1}. Under these conditions, DMDS is fully decomposed into H_2S.

2.3. Characterisation

2.3.1. Transmission electron microscopy (TEM)

TEM was carried out on a JEOL-120 CX at 100 kV. A VG HB5 scanning transmission electron microscope (STEM) equipped with a TRACOR TN524 energy dispersive X-ray spectrometer (X-EDS) was used for local analysis.

2.3.2. Infrared spectroscopy coupled with CO chemisorption IR(CO)

IR(CO) spectra were obtained on a DIGILAB FTS80 interferometer. The sample (20 mg) was pressed to a disk under 200 kg/m^2 and placed in an in situ cell. A thermal treatment was applied as follows: reduction under hydrogen at 450°C (2 h), cooling to 30°C under secondary vacuum (4×10^{-6} Torr), then at 30°C, introduction of 30 mbar of CO. Uniform distribution of CO molecules was obtained by heating the sample to 100°C for 15 min under CO pressure. The sample was then steadily heated under secondary vacuum at 30°C for 1 h and at 100, 240, 340, 380°C during 30 min until CO desorption was stabilised. After each step, spectra were obtained at room temperature in transmission mode (accumulation time = 100 s; resolution = 4 cm^{-1}).

2.3.3. Temperature programmed reduction (TPR)

TPR for sulfided metallic systems was performed on a modified χ-sorb apparatus. Catalysts were first sulfided 2 h at 400°C (5°C/min) with a mixture of 700 ppm H_2S/H_2. The reduction was performed with a 10°C/min heating ramp up to 900°C and allowed a coupled analyse of H_2 consumed and H_2S desorbed.

2.3.4. Extended X-Ray adsorption fine structure (EXAFS)

The EXAFS spectra at the Pd K-edge (24,352 eV), Ge K-edge (11,105 eV) and Pt L_{III}-edge (11,564 eV) for Pt–Ge/Al_2O_3, Pt–Pd/Al_2O_3 and sulfided Pt–Pd/Al_2O_3 were measured using a Si(1 1 1) crystal monochromator for Pt L_{III}-edge and a Si(3 1 1) crystal monochromator for Pd K-edge at the LURE synchrotron (Laboratoire d'Utilisation du Rayonnement Synchrotron, Orsay). All spectra were recorded in transmission mode at room temperature using an EXAFS cell with 4–6 mm of thickness. Data were analysed using a standard procedure [11]. Structural parameters (co-ordination numbers and interatomic distance) of the reference compounds used in this study were respectively (12, 2.76 Å for the Pt foil; 12, 2.75 Å for the Pd foil). Phases and amplitudes were calculated using theoretical files [12].

2.3.5. Low energy ion spectroscopy (LEIS)

LEIS was performed in an ESCALAB 200R from Fisons Instruments at IRC (Institut de Recherches sur la Catalyse, Villeurbanne). Catalysts Pt_xPd_y were studied after a 2 h reduction at 450°C under hydrogen. LEIS measurements were performed with 1 keV He^+ ions at a scattering angle of 142°. The intensity of the primary beam was fixed at 20 nA with an impact spot of around 0.2 mm^2. The ratio of sensitivity factors of Pt and Pd was determined by Cadrot [13] on monocrystals [1 1 1] of platinum and [1 0 0] of palladium as $S_{Pd}/S_{Pt} = 1.2$. The characteristic kinetic energies were approximately 880 eV for Pd and 930 eV for Pt.

Table 1
Orthoxylene hydrogenation rate with 100 ppm of S (operating conditions: LHSV $= 1\,h^{-1}$; $T = 200°C$)

Catalysts	Conversion (%)	Hydrogenation rate
Pt_1	3.5	3.0×10^{-3} mol h^{-1} g^{-1} Pt
$Pt_{50}Ge_{50}$	0	0×10^{-3} mol h^{-1} g^{-1} Pt
$Pt_{50}Pd_{50}$co	9.0	7.3×10^{-3} mol h^{-1} g^{-1} Pt
Pd_1	0.4	0.6×10^{-3} mol h^{-1} g^{-1} Pd

Table 2
TEM and X-EDS results

Catalysts	Surface average particle size (Å)	M/Pt (X-EDS results)
Pt_1	12	–
$Pt_{70}Ge_{30}$	12	–
$Pt_{90}Ge_{10}$	11.5	–
$Pt_{50}Ge_{50}$	11	0.3 ± 0.1
$Pt_{20}Pd_{80}$co	20	–
$Pt_{50}Pd_{50}$co	20	0.9 ± 0.2

3. Results

3.1. Aromatic hydrogenation with sulfur

The hydrogenation rate in presence of sulfur of $Pt_{50}M_{50}$ (atomic composition) has been compared to the monometallic platinum catalyst (Table 1). The hydrogenation rate is doubled for $Pt_{50}Pd_{50}$co reaching 7.3×10^{-3} mol h^{-1} g^{-1} Pt compared to 3.0×10^{-3} mol h^{-1} g^{-1} Pt for Pt_1. When germanium is added, a rapid deactivation is observed resulting in an activity close to zero in the measurement conditions (LHSV $=1\,h^{-1}$).

3.2. Charaterisation by TEM and X-EDS of bimetallic catalysts

Average surface particles sizes were evaluated by direct observation by TEM (Fig. 1), the quantitative determination of M/Pt ratio by X-EDS are also presented (Table 2). For the range of composition studied addition of germanium does not change the average metallic particle size (11 Å). Average particle size is a surface average size defined by $\sum n_i {d_i}^3 / \sum n_i {d_i}^2$ (n_i number of particle of diameter d_i). On the other hand, the average particle size of $Pt_{50}Pd_{50}$co catalysts is 20 Å showing an increase when compared to the starting Pt monometallic catalyst. Varying the Pd loading does not affect the average particle size. The local X-EDS analysis shows the bimetallic character of Pt–Pd particles (Table 2) for which the value is close to the nominal ratio. For Pt–Ge catalysts, the results indicate that metallic particles are deficient in Ge which is probably partially dispersed onto the support under monometallic form.

3.3. Study of the modification of electronic properties

The modification of electronic density of the metal has been investigated by IR(CO) chemisorption and catalytic hydrogenation of orthoxylene. The first technique enables the study of electronic effects through the frequency shift of the stretching vibration ν(CO) adsorbed linearly on platinum. To avoid dipole–dipole interactions, ν(CO) frequencies were measured at lowest CO coverage (close to zero). Wavenumber of CO adsorbed linearly on platinum at lowest CO coverage ν(CO) are given in Table 3. Addition of Ge

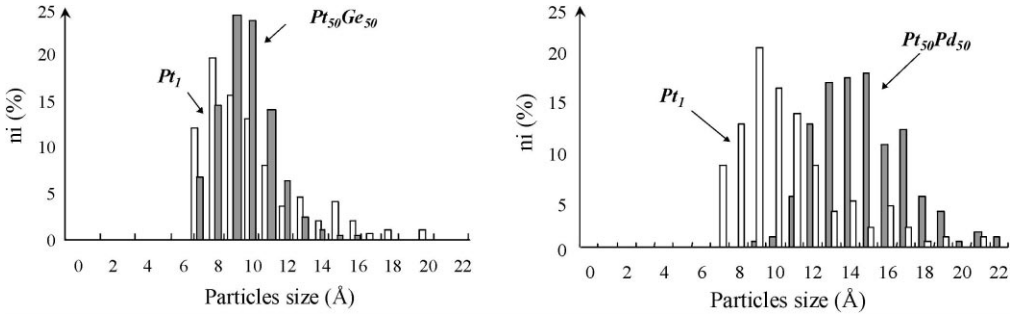

Fig. 1. TEM histogram of $Pt_{50}Ge_{50}$ and $Pt_{50}Pd_{50}$co.

Table 3
IR wavenumbers, selectivities toward *trans*-DMCH and conversion rate for orthoxylene hydrogenation

Catalysts	IR wavenumbers after desorption (cm^{-1})	Selectivity in *trans*-DMCH (%)	Conversion (%)	Hydrogenation rate
Pt_1	2039	31.2	6.1	230×10^{-3} mol h^{-1} g^{-1} Pt
$Pt_{50}Ge_{50}$	2051	48.0	0.1	10×10^{-3} mol h^{-1} g^{-1} Pt
$Pt_{50}Pd_{50}$	2032	43.0	0.8	30×10^{-3} mol h^{-1} g^{-1} Pt
Pd_1	2063	69.0	0.06	4×10^{-3} mol h^{-1} g^{-1} Pd

leads to a band wavenumber shift of $+12\,cm^{-1}$ (from $2039\,cm^{-1}$ for Pt_1 to $2051\,cm^{-1}$ for $Pt_{50}Ge_{50}$), interpreted as a decrease in electronic density of platinum atoms. Interpretation of the Pt–Pd catalyst results are more difficult because it has to be taken into account that Pd adsorbs CO. The adsorption frequencies of CO–Pt and CO–Pd species are close to one another and difficult to separate for Pt–Pd systems. The fact that spectra of bimetallic Pt–Pd presents some similarities with those of a pure Pd catalyst (presence of bridged species), suggests that the extreme surface of these particles is occupied only by palladium atoms as LEIS analysis will confirm (Section 3.6).

Orthoxylene hydrogenation has been described as a reaction sensitive to electronic density modification for metallic catalysts [14–16]. The hydrogenation of orthoxylene leads to *cis* and *trans* 1,2-dimethyl cyclohexane (DMCH) isomers which are favoured, respectively, by high and low electron density of the metallic centre. In our conditions, it has been checked that the *trans* isomer selectivity is not dependent on the conversion so that the discrepancy between the catalysts cannot be related to a kinetic effect. Hydrogenation rate (expressed as moles of orthoxylene transformed per gram of platinum and per hour) are presented in Table 3. The activity of the platinum catalysts decreases with addition of germanium and the *trans*-DMCH selectivity increases from 31% for Pt_1 to 48% for $Pt_{50}Ge_{50}$. This result suggests an electro-acceptor effect of germanium vis-à-vis platinum. For the $Pt_{50}Pd_{50}$co catalysts, the resultant activity is low and has been checked to be lower than the sum of specific Pt_1 and Pd_1 activities (no addition effect). The selectivity towards *trans* isomer is reduced compared with Pd_1 and can be interpreted by an increase of the electronic density of palladium atoms which could cover the surface of the particles.

Table 4
EXAFS results at Pt L_{III}-edge for Pt–Ge and Pt–Pd samples

Catalysts	Nearest neighbours	Distance (Å)	Debye–Waller factor $\Delta\sigma$ (Å)
Pt_1	Pt = 7.0	2.73	0.09
$Pt_{50}Ge_{50}$	Pt = 3.6	2.67	0.09
	Ge = 1.5	2.36	0.09
	O = 0.5	1.8	0.09
$Pt_{50}Pd_{50}$	Pt = 7.8	2.72	0.07
	Pd = 1.5	2.71	0.09
$Pt_{20}Pd_{80}$co	Pt = 7.8	2.73	0.08
	Pd = 4.0	2.67	0.08

3.4. Atomic structure: EXAFS measurements

Structural parameters (co-ordination numbers and interatomic distance) of the catalysts are reported in Tables 4 and 5. For the Pt_1 catalyst, the environment of a Pt atom consists of 7 other Pt atoms, located at a distance of 2.73 Å, close to the reference metal Pt distance. The environment of the Pt atoms is strongly modified in the presence of germanium. Pt, Ge and O atoms were found in the first co-ordination sphere of Pt. A significant reduction in the number of Pt neighbours is observed. (3.6 for 7).

Table 5
EXAFS results at Ge K-edge or Pd L_{III}-edge for Pt–Ge and Pt–Pd samples

Catalysts	Nearest neighbours	Distance (Å)	Debye–Waller factor $\Delta\sigma$ (Å)
$Pt_{50}Ge_{50}$	O = 7.2	2.67	0.09
$Pt_{50}Pd_{50}$	Pt = 4.2	2.82	0.09
	Pd = 2.8	2.61	0.10
$Pt_{20}Pd_{80}$co	Pt = 1.3	2.68	1.10
	Pd = 6.0	2.75	0.08

An average distance Pt–Ge of 2.36 Å between the germanium and platinum atoms corresponds to the Pt–Ge alloy distance (between 2.4 and 2.65 Å in the Pt_3Ge alloy). The presence of oxygen in the first co-ordination sphere of platinum after a 2 h reduction at 450°C is probably due to the metal support interface (Pt–O–Al bond). At germanium edge, only a bond Ge–O could be detected in agreement with the presence of a GeO_2 hexagonal structure (Ge–O = 1.73 Å). This result is in agreement with an oxidised state of the germanium, with only a small part of the Ge involved in Pt–Ge alloy formation.

For Pt–Pd catalysts, Pd and Pt atoms are present in metallic form at each metal edge representative of Pt–Pd alloy formation. Pd atoms are always lower co-ordinated than Pt suggesting a segregation of Pd at the bimetallic particle surface in agreement with the other characterisation results (IR(CO) and LEIS).

3.5. Analysis of the Surface by LEIS

The LEIS spectra of reduced catalysts $Pt_{50}Pd_{50}$co, $Pt_{30}Pd_{70}$co and $Pt_{20}Pd_{80}$co, at minimum erosion time (characteristic of surface composition) are presented in Fig. 2. The percentage of surface palladium is reported in Table 6. The surface Pd percentage is very high compared to relative atomic percentage (87% of surface palladium for $Pt_{50}Pd_{50}$co), indicating that the first layer is palladium-rich. Surface palladium enrichment increases with Pd/Pt ratio, confirming the EXAFS results. The $Pt_{20}Pd_{80}$co bimetallic particles have an eggshell (palladium shell, platinum core) structure.

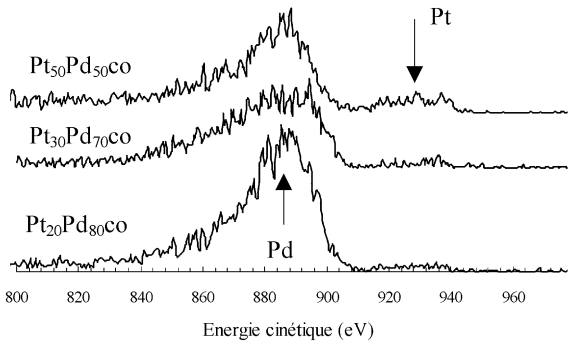

Fig. 2. LEIS spectra of Pt_xPd_yco catalysts (700–1000 eV — energy step 0, 6 eV).

Table 6
Percentage of surface palladium for Pt_xPd_yco

Catalysts	%Pd surface
$Pt_{50}Pd_{50}$co	87
$Pt_{30}Pd_{70}$co	95
$Pt_{20}Pd_{80}$co	98

3.6. Study of sulfur adsorption by programmed temperature reduction of sulfided catalysts

This technique was used to study the desorption of sulfur as H_2S for all sulfided catalysts (Fig. 3a and b). The production of H_2S for sulfided alumina was characterised by a large peak centred on 420°C. For sulfided Pt_1 catalyst, two major peaks of H_2S were recorded, centred on 440 and 610°C. The first was due to the sulfur desorption from the alumina support. The second one was ascribed to the reduction of a Pt–S species leading to H_2S. The calculated ratio S/Pt is 0.95, showing that the metallic platinum is fully sulfided.

The large H_2S desorption peak obtained for $Pt_{50}Ge_{50}$ (Fig. 3a) was interpreted as the sum of H_2S on alumina and H_2S due to the reduction of Pt–S species. The reduction of Pt–S is displaced to lower temperatures in presence of germanium: the strength of Pt–S bond is decreased, in agreement with an electro-deficient character of Pt in presence of germanium. For sulfided Pd_1 catalyst, two major peaks of H_2S were recorded (Fig. 3b), centred on 400 and 840°C. The first one was due to the sulfur present on alumina. The second one was attributed to the reduction of a Pd–S species. The production of H_2S for $Pt_{20}Pd_{80}$co is similar to Pd_1 with a small move to higher temperature (40°C).

3.7. EXAFS on sulfided systems

After catalytic tests in presence of sulfur, samples were analysed by EXAFS without exposure to air (Tables 7 and 8). In presence of sulfur, platinum loses its metallic character: for Pt_1S, the number of platinum atoms at Pt edge is decreased (7–1.6) and sulfur neighbours are observed. The Pt–S distance of 2.31 Å is coherent with a Pt–S bond [17]. For Pt_xPd_ySco, the EXAFS results are similar to Pt_xPd_yco after reduction

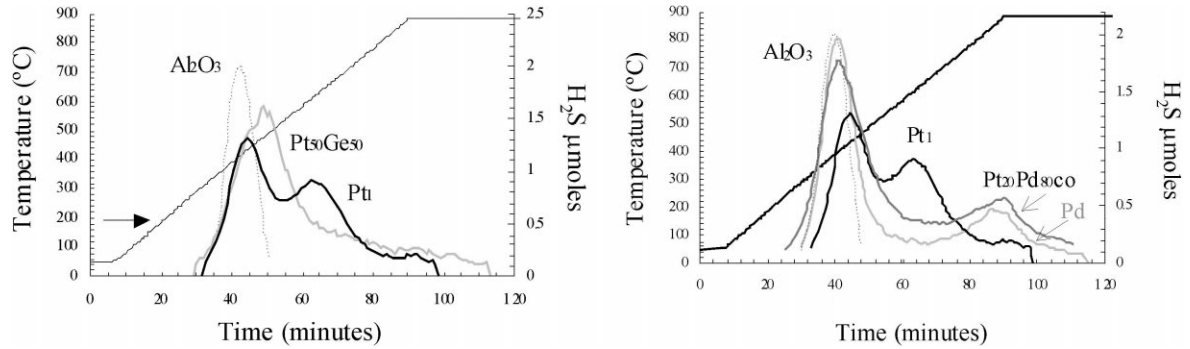

Fig. 3. (a) H_2S production during TPR of alumina, Pt_1, $Pt_{50}Ge_{50}$ after sulfidation; (b) H_2S production during TPR of alumina, Pt_1, Pd_1, $Pt_{20}Pd_{80}$co after sulfidation.

Table 7
EXAFS results Pt L_{III}-edge for Pt_1S, Pt–Pd–S

Catalysts	Nearest neighbours	Distance (Å)	Debye–Waller factor $\Delta\sigma$ (Å)
Pt_1S (1550 ppm S)	Pt = 1.6	2.73	0.08
	S = 3.7	2.30	0.08
$Pt_{50}Pd_{50}S$ (1900 ppm S)	Pt = 7.5	2.72	0.06
	Pd = 2.9	2.66	0.10
$Pt_{20}Pd_{80}Sco$ (2290 ppm S)	Pt = 10.0	2.72	0.08
	Pd = 2.2	2.65	0.10

without sulfur except for the presence of sulfur in the first co-ordination shell of palladium. The sulfur is not present at Pt edge: platinum keeps its metallic form in Pt–Pd systems.

4. Discussion

As shown by CO chemisorption coupled with IR and by orthoxylene hydrogenation, germanium acts as an electro-acceptor toward platinum and the strength of Pt–S bond is weakened (TPR). However and contrary to the usual literature hypothesis, addition of germanium to platinum fully inhibits aromatic hydrogenation activity in the presence of sulfur. In order to explain the non-sulfur resistance of Pt–Ge, one must take into account the modification of adsorption strength of hydrocarbons due to the variation of electronic density of surface atoms [18,19] according the Sabatier principle. As regards to Pt–Ge catalyst,

Table 8
EXAFS results at Pd L_{III}-edge for Pt–Pd–S samples

Catalysts	Nearest neighbours	Distance (Å)	Debye–Waller factor $\Delta\sigma$ (Å)
$Pt_{50}Pd_{50}S$ (1900 ppm S)	Pt = 5.0	2.69	0.10
	Pd = 1.6	2.76	0.09
	S = 0.6	2.32	0.06
$Pt_{20}Pd_{80}Sco$ (2290 ppm S)	Pt = 1.9	2.69	1.10
	Pd = 4.5	2.75	0.09
	S = 2.2	2.30	0.08

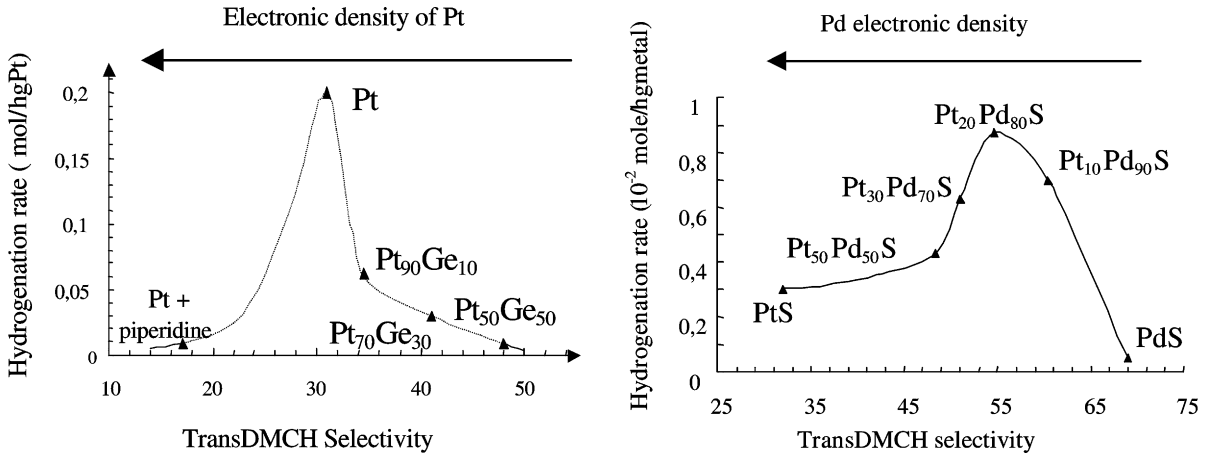

Fig. 4. Vulcano curves obtained with the Pt–Pd and Pt–Ge systems.

charge transfer from the aromatic nucleus is more important on an electro-deficient platinum and this strong adsorption is responsible for the self-inhibition of the reaction. In presence of an electro-acceptor element such as sulfur, platinum is even more electro-deficient and the phenomenon is emphasised. Concerning the Pt–Pd system, the $Pt_{20}Pd_{80}$ composition gave the best hydrogenation activity in presence of S. Characterisation shows that the active particles are formed by a Pd–S shell and Pt (sulfur free) core. Pt and S modify the electronic properties of surface Pd atoms (Pt increases the Pd electronic density with an increase of the Pd–S bond strength) leading to the optimum electronic configuration and the optimum aromatic adsorption strength under our operating conditions.

Fig. 4 presents for the two catalytic systems, the evolution of hydrogenation rate with the *trans*-DMCH selectivity (measured without sulfur) and related electronic density. An optimum was observed for Pt–Pd systems with varying particle composition (adjustment of aromatic adsorption on Pd–S–Pt): the maximum of orthoxylene hydrogenation rate in presence of sulfur is obtained for the $Pt_{20}Pd_{80}$co catalysts which roughly corresponds to the monolayer of palladium supported on platinum particles. Concerning Pt–Ge catalysts, by adding in the feed small amounts of piperidine which acts as an electro-donor, it has been possible to tune the adsorption properties and to describe the whole vulcano curve.

5. Conclusion

It has been shown in this work that the decrease of the M–S bond strength is not a sufficient condition to obtain high aromatic hydrogenation activity in presence of H_2S. Indeed, for given operating conditions, fine tuning of the electronic properties of the active site, obtained by good control of catalyst preparation, is required for optimal catalytic activity. A new sulfur resistant catalyst concept is proposed taking into account all the catalytic actor: an optimum can be found between all the conjugated effects: aromatic adsorption, sulfur adsorption, metallic phase properties (structure, surface composition, electronic modification) and support.

Acknowledgements

The author thanks P. Delichère, J.C. Bertolini from IRC (Villeurbanne) for LEIS experiments and fruitful discussions, Ph. Dascotte and N. Zanier (IFP) for MET and IR(CO) experiments, respectively.

References

[1] P. Gallezot, J. Dakta, J. Massardier, M. Primet, B. Imelik, Proceedings of the Sixth ICC, Vol. 2, The Chemical Society, London, 1977, p. 696.
[2] C. Song, D. Schmitz, Energy and Fuels 11 (1997) 656–661.

[3] J.T. Miller, D.C. Koninsberger, J. Catal. 162 (1996) 202–219.
[4] T.B. Lin, C.A. Jan, J.R. Chang, Ind. Eng. Chem. Res. 34 (1995) 4284–4289.
[5] A. Borgna, T.F. Garetto, A. Monzon, R. Apesteguia, Stud. Surf. Sci. 101 (1996) 1155.
[6] J. Oudar, Metal support and metal additive effect in catalysis, Stud. Surf. Sci. 11 (1982) 255.
[7] P. Gallezot, Catal. Rev. Sci. Eng. 20 (1) (1980) 201.
[8] N.S. Figoli, P.C. L'Argentiere, Catal. Today 5 (1989) 403.
[9] T.M. Tri, J. Massardier, Stud. Surf. Sci. 5 (1980) 279–284.
[10] E. Merlen, P. Beccat, J.C. Bertolini, P. Delichère, N. Zanier, B. Didillon, J. Catal. 1598 (1996) 178–188.
[11] D. Bazin, H. Dexpert, J.P. Bournonvillle, J. Lynch, J. Catal. 123 (1990) 86.
[12] A.G. McKale, B.W. Veal, A.P. Panlikas, S.K. Chan, G.S. Knapp, J. Am. Chem. Soc. 110 (1988) 763.
[13] A.M. Cadrot, Thèse, Université de Lyon, 1998.
[14] K. Chandes, B. Didillon, Communication Europacat, Montpellier, 1993.
[15] M. Vinegria, G. Cordoba, R. Gomez, J. Mol. Catal. 58 (1990) 107.
[16] G. Del Angel, Trompantzi, R. Gomez, React. Kinet. Catal. Lett. 42 (1) (1990) 67–72.
[17] F.A. Banister, M.H. Hey, J. Miner. Soc. 23 (1932) 188.
[18] J. Cosyns, Catalyse par les Métaux, Editions du CNRS, Paris, 1984, p. 371.
[19] J.P. Boitiaux, J. Cosyns, S. Vasudevan, Stud. Surf. Sci. Catal. 16 (1982) 123.